ChemComm

COMMUNICATION

View Article Online
View Journal

Check for updates

Cite this: DOI: 10.1039/d4cc05384b

Received 11th October 2024,
Accepted 2nd December 2024

DOI: 10.1039/d4cc05384b

rsc.li/chemcomm

Published on 02 December 2024. Downloaded by Universidade de Aveiro (UAveiro) on 12/12/2024 2:01:29 PM.

Separation of metals using *in situ* formation of DES–DES biphasic systems†

André Nogueira, ‡[a] Camila Vallejos-Michea,‡[b] Sara Fateixa, [a] Yecid P. Jimenez,[bc] João A. P. Coutinho [a] and Nicolas Schaeffer *[a]

A biphasic system composed of two deep eutectic solvents (DES) sharing a common hydrogen-bond donor exhibits a tuneable phase behavior and efficient metal partitioning, yielding an improved separation selectivity of trivalent from divalent metal ions compared to the equivalent aqueous system.

Increased consumption and the emergence of sustainable technologies places a renewed emphasis on metal separation, both for their production and recycling. Solvent extraction is the preferred method for the separation and purification of metals from complex leachates due to its selectivity and ability to produce high purity metal salts.[1] However, the large volumes of often flammable and toxic solvents used raise environmental concerns. Furthermore, solvent extraction from aqueous leachates often relies on the media ionic strength or pH, depending on the nature of the extractant, making the efficient separation of ions with similar speciation challenging.[2] Replacement of the polar phase in solvent extraction by polar molecular or ionic solvents provides an opportunity to fine-tune the separation by harnessing the differences in metal ion solvation between water and organic solvents.[3]

Deep eutectic solvents (DES) incorporating hydrogen bond donors (HBD) with acidic groups along with a halide hydrogen bond acceptors (HBA), typically choline chloride (ChCl), significantly extended the potential for selective leaching of critical metals due to the change in coordination environment, making DES an attractive alternative to aqueous leaching agents.[4,5] However, the recovery of metals from DES is not straightforward and remains a significant hurdle to their implementation. For metals difficult to electrodeposit, this often requires the addition of a co-solvent to disturb the DES metal–ligand complex, most often water, followed by precipitation and distillation of the co-solvent prior to reuse, rendering DES recycling difficult and expensive.[6–8] Non-aqueous solvent extraction was previously applied for metal separation from DES with success.[3,9] However, as DES are not pure solvents but mixtures, the potentially high mutual miscibility of at least one of the DES components in the apolar phase can lead to a cost-ineffective process due to the resulting change in the phase composition after each processing cycle.[9,10] To benefit from the change in metal ion partition behaviour in non-aqueous solvents whilst minimizing the system complexity, in this work, a new solvent extraction methodology is proposed, exploiting the *in situ* formation of a biphasic DES–DES system.

The ability to form biphasic DES–DES systems using only three components was assessed by preparing ternary mixtures of a non-ionic hydrophobic metal extractant, trioctylphosphine oxide (TOPO), with ChCl, and an organic acid. A full description of the experimental protocol is available in the ESI† and Tables S1, S2. To facilitate the selection of the studied systems, we focused on ternary systems for which the binary systems phase diagrams are available and form liquid solutions at room temperature. Mixtures of TOPO with malonic acid (MA), levulinic acid, or butyric acid, were characterised and applied for the solvent extraction of Ga(III) or Pt(IV).[11,12] Likewise, DES formed by ChCl and short chain organic acids are effective leaching media for the dissolution of metal oxides.[4,13] A selection of six organic acids are here employed as HBD, namely malonic, levulinic, propionic, butyric, lactic, and acetic acid. While all form biphasic systems at room temperature (298 K), as shown in Fig. S1 and Tables S3–S7 (ESI†), MA-based DES systems were chosen to exemplify the potential of DES–DES system for separation.

The ternary phase diagram of the TOPO–ChCl–MA system is available in Fig. 1A and Table S8 (ESI†) and shows a narrow biphasic (LL) region only found in mixtures containing x_{MA} = 0.4 to 0.5. However, mixtures containing either x_{TOPO} and x_{ChCl} of 0.1 to 0.5 can form biphasic systems, demonstrating

[a] CICECO – Aveiro Institute of Materials, Department of Chemistry, University of Aveiro, 3810-193 Aveiro, Portugal. E-mail: nicolas.schaeffer@ua.pt
[b] Departamento de Ingeniería Química y Procesos de Minerales, Facultad de Ingeniería, Universidad de Antofagasta, Av. Angamos 601, Antofagasta, Chile
[c] Centro de Economía Circular en Procesos Industriales (CECPI), Facultad de Ingeniería, Universidad de Antofagasta, Av. Angamos 601, Antofagasta, Chile

† Electronic supplementary information (ESI) available. See DOI: https://doi.org/10.1039/d4cc05384b

‡ These authors contributed equally to this work.

Published on 02 December 2024. Downloaded by Universidade de Aveiro (UAveiro) on 12/12/2024 2:01:29 PM.

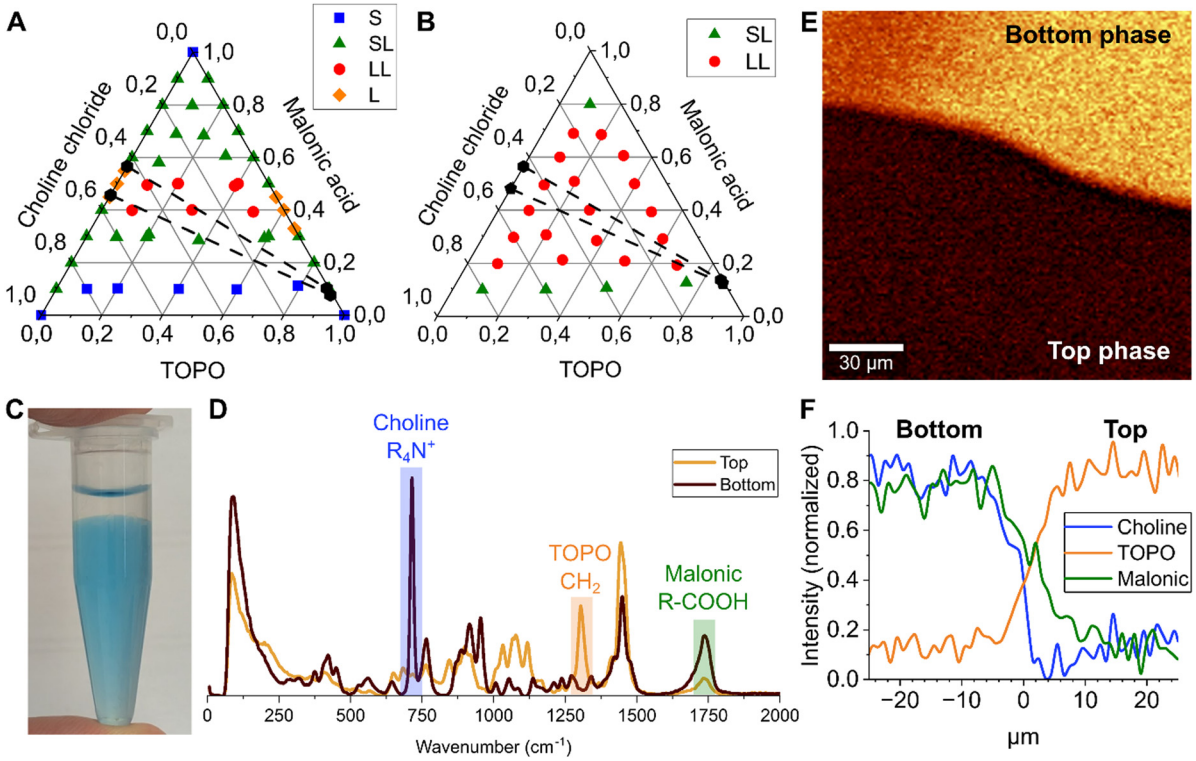

Fig. 1 (A) Phase diagram for the ternary system at 298 K with experimentally measured tie-lines indicated as black dashed lines. Mixture points are described as completely solid (S), a solid–liquid equilibrium (SL), as a biphasic liquid (LL) or as a homogenous liquid phase (L). Data for the binary TOPO–MA and ChCl–MA were taken from ref. 11 and 14. (B) Phase diagram of the ternary system with 10 wt% added water; (C) appearance of a system of x_{TOPO} = 0.1, x_{MA} = 0.5, and x_{ChCl} = 0.4. ChCl-rich phase is colored with E133 and E122 food dyes; (D) Raman spectra of the top and bottom phases after separation in the absence of added water; (E) two-dimensional Raman map across the interface integrating the area of the choline's Raman band at 712 cm^{-1}; (F) normalized intensity of specific Raman bands for choline (blue), TOPO (orange) and malonic acid (green) across the interface of the biphasic system.

some flexibility in system composition and potential for tuning to separation purposes. Moreover, the ternary equilibrium data shows good agreement with literature data for the individual TOPO–MA and ChCl–MA systems. TOPO–MA and ChCl–MA form liquid mixtures for x_{MA} = 0.3–0.5 and x_{MA} = 0.4–0.6 respectively as shown in Fig. 1A.[11,14] The binary miscibility windows overlap with the biphasic window of the ternary system, suggesting that the formation of ternary biphasic systems is contingent upon the binary DES components having compatible miscibility ranges. Additionally, a difference in the size, hence polarity, of the HBA appears to be essential for promoting phase separation as was observed for ionic liquid-ionic liquid biphasic systems.[15] Due to the common practice of adding small quantities of water to DES during lixiviation to improve mass transfer, the same system was studied after the addition of 10 wt% H_2O. A stark change in the phase diagram, Fig. 1B (Table S9, ESI†), is observed with an important widening of the biphasic region and near disappearance of the solid–liquid (SL) region for intermediate mole fraction of MA. The presence of small water concentrations in the system allows for a more forgiving biphasic system formation while also enabling easier handling and processing of the system. A significant reduction of the ChCl-rich phase viscosity from 1023 mPa s to a manageable 83.3 mPa s was observed upon addition of 10 wt% H_2O (Tables S10 and S11, ESI†).

Tie-lines for the system with and without 10 wt% H_2O are measured experimentally (full details in Tables S10, S11 and Fig. S2–S6, ESI†), and shown as dashed lines in Fig. 1A and B. They indicate the almost complete exclusion of TOP and ChCl from their opposite respective phase, whilst MA partitions preferentially to the ChCl phase. The addition of 10 wt% H_2O has a negligible effect on the tie-lines. A more detailed discussion of the tie-lines is available in the corresponding section of the ESI.† Raman spectroscopy supplements the phase composition results, analysing a system of overall composition x_{TOPO} = 0.1, x_{MA} = 0.5, and x_{ChCl} = 0.4, depicted in Fig. 1C. The Raman spectra of each phase at equilibrium are presented in Fig. 1D, along with the characteristic bands of each compound followed (see Table S12 for the principal Raman bands assignment, ESI†). Fig. 1E displays a two-dimensional Raman map of a 150 μm^2 cross-section along the liquid–liquid interface. The lighter the colour, the higher is the intensity of the 712 cm^{-1} peak assigned to the C–N symmetric stretching mode for the *gauche* conformations of the O–C–C–N^+ backbone. By plotting the normalised intensity of the respective characteristic bands shown in Fig. 1D, the evolution of each compound along the biphasic system (*z*-direction) can be determined, as shown in Fig. 1F. The Raman results confirm the almost complete partition of TOPO and ChCl to opposite phases in the ternary system and minimal contamination of the phases resulting from the

 This journal is © The Royal Society of Chemistry 2024

Published on 02 December 2024. Downloaded by Universidade de Aveiro (UAveiro) on 12/12/2024 2:01:29 PM.

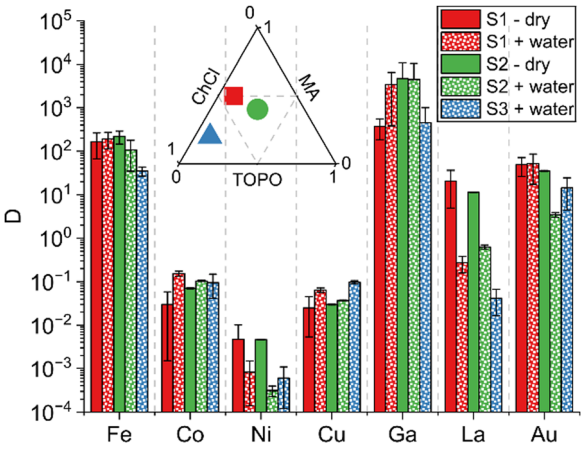

Fig. 2 Distribution coefficient (*D*) for three different mixture points with and without added water. The system composition is provided in the inset phase diagram along with the colour code. All *D* values are available in Table S13 (ESI†).

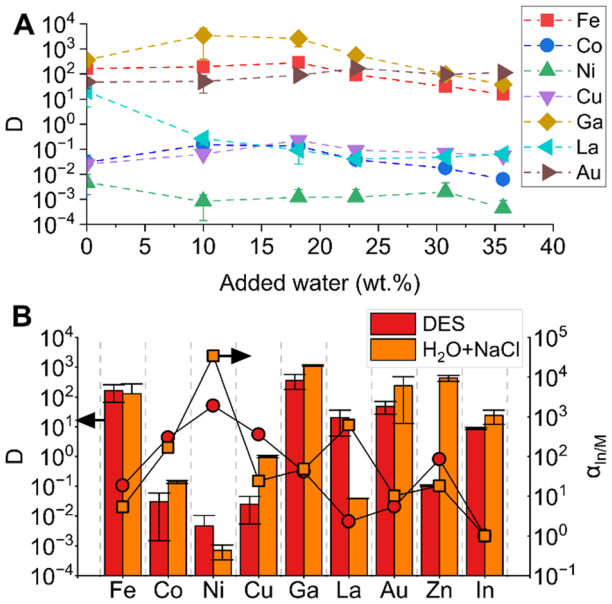

Fig. 3 (A) Metal ion distribution factor as a function of the water content for a system with initial composition x_{TOPO} = 0.1, x_{MA} = 0.5, x_{ChCl} = 0.4. (B) Difference in metal ion distribution (bars) and In(III)/M separation factor (lines) between a DES–DES (same composition as in (A)) and DES-aqueous (x_{TOPO} = 0.9, x_{MA} = 0.1) system for an equal chloride concentration of 4.65 mol L^{-1}. All *D* values are available in Tables S15 and S16 (ESI†).

combination of all three compounds. Interestingly, a greater penetration of MA to the TOPO-rich phase relative to ChCl is observed, hinting at its interfacial accumulation in the biphasic system and its stabilising influence on the more apolar phase.

Following its characterisation, the capacity of the biphasic system for metal separation is assessed. Three different mixture points were spiked with aqueous chloride solutions of Fe(III), Co(II), Ni(II), Cu(II), Ga(III), La(III) and Au(III). These chloride salts were selected as representative of various classes of metal ions. Fig. 2 and Table S13 (ESI†) show the distribution coefficient (*D*) for selected biphasic systems with and without 10 wt% H_2O addition, whose compositions are displayed in the inset phase diagram. The divalent Co(II), Ni(II) and Cu(II) distribute preferentially to the ChCl-rich phase (bottom), whereas trivalent Fe(III), Ga(III) and Au(III) partition to the TOPO-rich phase. Except for La(III), phase composition was found to play a minor role in metal separation as all three selected systems showed similar metal partitioning. The extraction kinetics for the dry System 1 in Fig. 2 (x_{TOPO} = 0.1, x_{MA} = 0.5, x_{ChCl} = 0.4) is presented in Fig. S7 and Table S14 (ESI†). Despite the high viscosity of the ChCl-rich phase, the system presented a reasonably rapid extraction with only 10 min of moderate agitation required to reach equilibrium.

The change in the La(III) distribution coefficient when transitioning between dry and wet systems prompts a more thorough study of the role of water content on the metal partition. System 1 in Fig. 2 is selected to better understand the role of metal speciation in the extraction. Increasing amounts of water was added and metal distribution measured – Fig. 3A and Table S15 (ESI†) – and is complemented by the change in the UV-vis spectra of the ChCl-rich phase under the same extraction conditions, Fig. S8 (ESI†). In the "dry" system, the peak at 400 nm is assigned to $CuCl_4^{2-}$ complexes,[16] whilst the three bands at 630, 660 and 690 nm correspond to the spectrum of $CoCl_4^{2-}$.[17] The UV-VIS spectrum of the TOPO-rich phase, available in Fig. S9 of the ESI,† reveals the presence of the $FeCl_4^-$ chlorocomplex. Ni(II) and La(III) are unlikely to form anionic complexes even at very high Cl^- concentrations as M^+–Cl^- interactions do not dominate in these systems,[18,19] whereas Ga(III) and Au(III) are expected to exist as $GaCl_4^-$ and $AuCl_4^-$, respectively.[20,21] Except for La(III), only anionic species of total charge −1 migrate to the TOPO-rich phase. The co-extraction of $[Ch]^+$ to the TOPO-rich phase, necessary to maintain charge balance, provides an energetic penalty to the partitioning of anionic complexes, minimising the extraction of $[MCl_4]^{2-}$ relative to $[MCl_4]^-$ species. This mechanism can be exploited for the selective separation of metals based on their valence. As TOPO is a solvating type extractant, the distribution of La(III) under "water-free" conditions is assigned to the favourable interaction between the electronegative P=O group of TOPO and the cation centre.[22] The decrease in intensity of the UV-vis band of anionic chlorocomplexes in Fig. S8 (ESI†) with water addition signals a shift in metal speciation from chloro-complexes to increasingly hydrated neutral or cationic metal species. This results in a strong decrease in La(III) distribution, and, to a lesser extent Fe(III) and Ga(III) with increasing dilution, although Au(III) partition remains unaffected. Beyond improving the phase separation properties and lowering viscosity, the presence of small quantities of added water can further tune the selectivity.

As a proof of concept, the separation of In(III), Ga(III) and Zn(II) from the ChCl–MA DES is attempted using system 1, mimicking the metals present during the recycling of IGZO semiconductors. This system proves useful for the extraction of Ga(III) and In(III) (*D* of 369 and 8.97, respectively), leaving Zn(II) in the ChCl phase (D_{Zn} = 0.10). The results align with the separation mechanism proposed, as the monoanionic $GaCl_4^-$ and $InCl_4^-$ partition to the TOPO phase, leaving Zn(II), in the form of $ZnCl_4^{2-}$, in the ChCl-rich phase. Metal separation using

Published on 02 December 2024. Downloaded by Universidade de Aveiro (UAveiro) on 12/12/2024 2:01:29 PM.

this TOPO–ChCl–MA system is compared with an equivalent biphasic system composed of TOPO–MA but where the polar phase is an aqueous NaCl solution with $[Cl^-]$ = 4.65 mol L^{-1}, the same concentration as in the ChCl phase. The metal partition results, available in Fig. 3B and Table S16 (ESI†), show an improved metal separation in the DES–DES system when compared to the DES-aqueous system. In the case of IGZO recycling, the DES–DES system is able to separate Zn(II) from In(III) and Ga(III), resulting in a separation factor (α) of $\alpha_{Ga(III)/Zn(II)} = 3.5 \times 10^3$ and $\alpha_{In(III)/Zn(II)} = 85$, compared to $\alpha_{Ga(III)/Zn(II)} = 2.6$ and $\alpha_{In(III)/Zn(II)} = 18$ obtained in the aqueous system.

Extending the comparison to the other metals in this study, the DES–DES system offers significantly improved selectivity in separating most trivalent metals from divalent ones compared to the equivalent aqueous NaCl system. For example, a $\alpha_{In(III)/Cu(II)}$ of 357 and 24 were obtained in the DES–DES and DES–NaCl system respectively. The latter is similar to that obtained when separating In(III) aqueous chloride media using quaternary ionic liquids as apolar phase, yielding $\alpha_{In(III)/Cu(II)}$ and $\alpha_{In(III)/Zn(II)}$ of approximately 6.1 and in the range of 0.06 to 0.58, respectively.[23] Direct reuse of the TOPO-rich phase (Fig. S10 and Table S17, ESI†) is possible at least 3 times with minimal changes in selectivity. Although preliminary, separation of the extracted Fe(III), Ga(III), In(III), and Au(III) ions (based on the results in Fig. 3A) can be achieved *via* selective stripping of Fe(III) and Ga(III) with dilute H_2SO_4 (pH = 2) or Ga(III) using 0.1 mol L^{-1} oxalic acid, summarised in Fig. S11 and Table S18 (ESI†), yielding a $\alpha_{In(III)/Ga(III)}$ in the range of 271–1353 depending on the strip solution. Partial recovery of Au(III) is obtained using 5 mol L^{-1} HCl, with more work required to improve the stripping of In(III). Finally, the stability of the regenerated phase after partial stripping with H_2SO_4 at pH = 2 is confirmed by NMR (Fig. S12, ESI†), with no changes relative to the as-prepared phase observed.

The *in situ* formation of a biphasic DES–DES system offers an enhanced and tuneable approach for selective metal separation. Characterization *via* visual observation, NMR and Raman spectroscopy offer insights into its phase behaviour and provides guidelines for the optimisation of analogous systems. Notably, the addition of small amounts of polar molecules (water in this case) helps widen the biphasic region, enabling nuanced separation with increased selectivity due to the unique driving forces for metal partitioning in non-aqueous media. Further work is required to extend the applicability of the proposed approach.

This work was co-funded by the European Union ERC-StG, DESignSX, (project 101116461). This work was partly developed within the scope of the project CICECO – Aveiro Institute of Materials, UIDB/50011/2020 (DOI: **https://doi.org/10.54499/UIDB/50011/2020**), UIDP/50011/2020 (DOI: **https://doi.org/10.54499/UIDP/50011/2020**) & LA/P/0006/2020 (DOI: **https://doi.org/10.54499/LA/P/0006/2020**), financed by national funds through the FCT/MCTES (PIDDAC). A. N. and S. F. acknowledge FCT, I.P., for the PhD grant 2023.01418.BD and research contract REF-069-88-ARH-2018 funded by national funds (OE) in the scope of the framework contract foreseen in the numbers 4, 5, and 6 of the article 23, of the Decree-Law 57/2016, of August 29, changed by Law 57/2017, of July 19, respectively. Y. P. J. and C. V. M. thank the Universidad de Antofagasta, the doctoral program in mineral process engineering, and ANID-Chile (No. 21221050) for funding this research through the FONDECYT (No. 1221428) project.

Data availability

The data supporting this article is included in the ESI.†

Conflicts of interest

There are no conflicts to declare.

References

1 A. M. Wilson, P. J. Bailey, P. A. Tasker, J. R. Turkington, R. A. Grant and J. B. Love, *Chem. Soc. Rev.*, 2013, **43**, 123–134.
2 F. Xie, T. A. Zhang, D. Dreisinger and F. Doyle, *Miner. Eng.*, 2014, **56**, 10–28.
3 Z. Li, B. Dewulf and K. Binnemans, *Ind. Eng. Chem. Res.*, 2021, **60**, 17285–17302.
4 M. I. Martín, I. García-Díaz and F. A. López, *Miner. Eng.*, 2023, **203**, 108306.
5 P. G. Schiavi, P. Altimari, E. Sturabotti, A. Giacomo Marrani, G. Simonetti and F. Pagnanelli, *ChemSusChem*, 2022, **15**, e202200966.
6 P. Zürner and G. Frisch, *ACS Sustainable Chem. Eng.*, 2019, **7**, 5300–5308.
7 G. Ji, D. Tang, J. Wang, Z. Liang, H. Ji, J. Ma, Z. Zhuang, S. Liu, G. Zhou and H.-M. Cheng, *Nat. Commun.*, 2024, **15**, 4086.
8 X. Chang, M. Fan, C.-F. Gu, W.-H. He, Q. Meng, L.-J. Wan and Y.-G. Guo, *Angew. Chem., Int. Ed.*, 2022, **61**, e202202558.
9 S. Spathariotis, N. Peeters, K. S. Ryder, A. P. Abbott, K. Binnemans and S. Riaño, *RSC Adv.*, 2020, **10**, 33161–33170.
10 J.-B. Chagnoleau, N. Papaiconomou, M. Jamali, D. O. Abranches, J. A. P. Coutinho, X. Fernandez and T. Michel, *ACS Sustainable Chem. Eng.*, 2021, **9**, 9707–9716.
11 E. L. Byrne, R. O'Donnell, M. Gilmore, N. Artioli, J. D. Holbrey and M. Swadźba-Kwaśny, *Phys. Chem. Chem. Phys.*, 2020, **22**, 24744–24763.
12 R. Liu, Y. Geng, Z. Tian, N. Wang, M. Wang, G. Zhang and Y. Yang, *Hydrometallurgy*, 2021, **199**, 105521.
13 Y. Wen, X. He, S. Di, K. Liu, D. Li and J. Du, *J. Environ. Chem. Eng.*, 2023, **11**, 110979.
14 E. A. Crespo, L. P. Silva, M. A. R. Martins, M. Bülow, O. Ferreira, G. Sadowski, C. Held, S. P. Pinho and J. A. P. Coutinho, *Ind. Eng. Chem. Res.*, 2018, **57**, 11195–11209.
15 S. Omar, J. Lemus, E. Ruiz, V. R. Ferro, J. Ortega and J. Palomar, *J. Phys. Chem. B*, 2014, **118**, 2442–2450.
16 W. Liu, A. Migdisov and A. Williams-Jones, *Geochim. Cosmochim. Acta*, 2012, **94**, 276–290.
17 M. Uchikoshi, *J. Solution Chem.*, 2018, **47**, 2021–2038.
18 J. T. M. Amphlett, Y. Lee, W. Yang, D. Kang, N.-E. Sung, J. Park, E. C. Jung and S. Choi, *ACS Omega*, 2022, **7**, 921–932.
19 J. M. Hartley, C.-M. Ip, G. C. H. Forrest, K. Singh, S. J. Gurman, K. S. Ryder, A. P. Abbott and G. Frisch, *Inorg. Chem.*, 2014, **53**, 6280–6288.
20 C. Hardacre, R. W. Murphy, K. R. Seddon, G. Srinivasan and M. Swadźba-Kwaśny, *Aust. J. Chem.*, 2010, **63**, 845–848.
21 J. A. Peck, C. D. Tait, B. I. Swanson and G. E. Brown, *Geochim. Cosmochim. Acta*, 1991, **55**, 671–676.
22 B. Dewulf, V. Cool, Z. Li and K. Binnemans, *Sep. Purif. Technol.*, 2022, **294**, 121197.
23 C. Deferm, M. V. de Voorde, J. Luyten, H. Oosterhof, J. Fransaer and K. Binnemans, *Green Chem.*, 2016, **18**, 4116–4127.

 This journal is © The Royal Society of Chemistry 2024